

Difficulty in Determining the Pion Form Factor at High Q^2

C. E. Carlson and Joseph Milana

Physics Department, College of William and Mary, Williamsburg, Virginia 23185

(Received 4 May 1990)

We reexamine the determination of the pion form factor at large spacelike Q^2 via the reaction $ep \rightarrow en\pi^+$ and find that, because of the magnitude of the pion-nucleon form factor and the existence of competing hitherto uncalculated processes in QCD, the pion electromagnetic form factor is not sufficiently well determined at higher Q^2 to compare with the expected scaling prediction of QCD. Instead, we conclude that the best way to get information about the pion electromagnetic form factor is to study π^0 production.

PACS numbers: 13.40.Fn, 12.38.Bx, 13.60.Le

Pion electroproduction can be calculated using meson and nucleon pole diagrams. Such calculations are used in determining the pion electromagnetic form factor at moderate to high momentum transfers,¹ using data from $ep \rightarrow en\pi^+$. Pion electroproduction may also be calculated reliably at high enough momentum transfers using perturbative quantum-chromodynamics (PQCD) and quark-gluon diagrams. The PQCD diagrams produce a background to the pion pole and other pole diagrams that could undermine the extraction of the pion form factor from the π^+ data. On the other hand, the PQCD diagrams may be the chief source of π^0 production. There is very little contribution to π^0 production from the pole diagrams. The contribution from the PQCD diagrams is proportional to the same integral over the pion wave function that determines the pion electromagnetic form factor at high momentum transfers,²⁻⁴ so that the best way to measure the pion form factor at these momentum transfers, albeit indirectly, may be to measure the electroproduction of π^0 .

Results for the pion electromagnetic form factor at moderate or high spacelike momentum transfers come from^{1,5}

$$e + p \rightarrow e + \pi^+ + n. \quad (1)$$

The data are analyzed in terms of nucleon and pion pole diagrams, shown in Fig. 1, and if the kinematics are chosen so that the variable $|t|$ [$t = (p - p')^2$] is small, one argues that the pion pole diagram, Fig. 1(t), dominates and the measured result depends only on known kinematic factors and the form factor $g_{\pi NN}(t)$ evaluated near $t=0$ and the pion electromagnetic form factor $F_\pi(Q^2)$ (where $q^2 = -Q^2$ is the four-momentum squared of the virtual photon). Taking $g_{\pi NN}(0)$ from

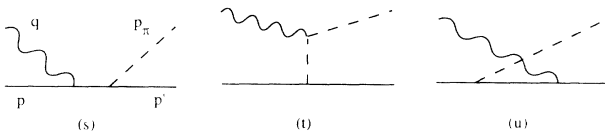


FIG. 1. The pion and nucleon pole graphs.

pion-nucleon scattering a value for $F_\pi(Q^2)$ is thus extracted and for $1 \text{ GeV}^2 \leq Q^2 \leq 4 \text{ GeV}^2$ (where the upper bound reflects limits set by the experimenters themselves) is found to be consistent with the expected power-law dependence predicted by PQCD,⁶ $F_\pi(Q^2) \propto 1/Q^2$.

This analysis is subject to criticisms which question whether F_π has been truly determined for large Q^2 . These criticisms stem from the size of $|t|$ and from the calculated size of competing reaction mechanisms. We wish to discuss these points, the second named one in some detail, and later will attempt to turn our discussion to positive use.

An immediate problem is that $|t|$ is not strictly zero, and this is serious in view of the current debate over the softness^{7,8} of $g_{\pi NN}$. For a given Q^2 and final c.m. energy W , and minimizing $|t|$ by having \mathbf{p}_π parallel to \mathbf{q} , we have

$$-t_{\min} = 2(E_1^* E_2^* - p_1^* p_2^* - m_N^2) \approx \frac{m_N^2 Q^4}{W^2(W^2 + Q^2)}, \quad (2)$$

where

$$E_1^* = (1/2W)(W^2 + m_N^2 + Q^2) = (m_N^2 + p_1^{*2})^{1/2}, \quad (3)$$

$$E_2^* = (1/2W)(W^2 + m_N^2 - m_\pi^2) = (m_N^2 + p_2^{*2})^{1/2}.$$

For example, the data point at $Q^2 = 3.33 \text{ GeV}^2$ and $W = 2.63 \text{ GeV}$ has $-t = 0.16 \text{ GeV}^2$. As the mass parameter in the monopole representation

$$g_{\pi NN}(t) = g_{\pi NN}(0)(1 - t/\Lambda_{\pi N}^2)^{-1} \quad (4)$$

ranges from a recently suggested⁸ $\Lambda_{\pi N} = 0.4 \text{ GeV}$ to something large, it induces a factor-of-2 change in the extracted $F_\pi(Q^2)$. Such ambiguity is clearly unfortunate in comparing with the predictions of PQCD for F_π at this Q^2 .

At large Q^2 , perturbative QCD introduces competing reaction mechanisms. An important such mechanism⁹ is shown in Fig. 2. (If the photon and pion attach to different quarks, there will be transverse momentum mismatches in the final state with consequent suppres-

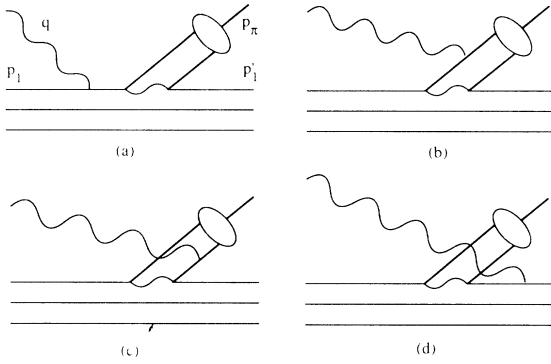


FIG. 2. The PQCD diagrams for our kinematics.

sion by powers of Q^2 .) We will calculate these diagrams and compare their size to the pole diagram of Fig. 1(t).

A question of double counting may arise, so let us comment about it now. Certain cuts of Fig. 2 have a superficial similarity to Fig. 1 [e.g., cutting the upward-going quark lines in Fig. 2(b) above the gluon but below the photon gives a quark pair that looks somewhat like the t -channel pole of Fig. 1(t)], but the intermediate states selected by these cuts have quarks with greatly mismatched momenta and so little overlap with any particular hadron state. Hence there is little overcounting and we can meaningfully compare calculations of Figs. 1 and 2. The nonoverlap is emphasized by, for example, noting later that Figs. 2(a) and 2(b) have the same magnitude whereas Figs. 1(s) and 1(t) are very different.

We work in the $q^+ = 0$ frame, where $p^\pm = p^0 \pm p^3$ and

$$\begin{aligned}
 p &= (p^+, p^-, p_T) = \left(p^+, \frac{m_N^2}{p^+}, 0_T \right), \\
 q &= \left(0, \frac{2m_N v}{p^+}, q_T \right), \\
 p_\pi &= \left(zp^+, \frac{p_{\pi T}^2 + m_\pi^2}{zp^+}, p_{\pi T} \right).
 \end{aligned}
 \tag{5}$$

One finds

$$-t = [z^2 m_N^2 + (q_T - p_{\pi T})^2] / (1-z). \tag{6}$$

The PQCD calculations are simplest if the outgoing proton has zero transverse momentum like the incoming proton, so that $p_{\pi T} = q_T$. The center-of-mass angle between the photon and pion is not then zero, but for the smaller z is compatible with the range of angles used in the data analysis of Ref. 1.¹⁰ We now have

$$\begin{aligned}
 p_\pi &= \left(zp^+, \frac{q_T^2 + m_\pi^2}{zp^+}, q_T \right), \\
 p' &= \left((1-z)p^+, \frac{m_N^2}{(1-z)p^+}, 0_T \right),
 \end{aligned}
 \tag{7}$$

and

$$z = \frac{Q^2 - t + m_\pi^2}{2m_N v} \gtrsim x = \frac{Q^2}{2m_N v}. \tag{8}$$

Thus to further shrink t to zero requires $x \rightarrow 0$, or big v for a given Q^2 .

At the single-quark level the PQCD amplitude for pion production is

$$\begin{aligned}
 \mathcal{M}_q &= - (2\lambda) \frac{4\pi\alpha_s C_F}{\sqrt{N_c}} [8(1-z)y_1 y_1']^{1/2} \\
 &\times \left[e_1 \frac{\varepsilon \cdot p}{q \cdot p_1'} + e_2 \frac{\varepsilon \cdot p}{q \cdot p_1} \right] I_\pi,
 \end{aligned}
 \tag{9}$$

where λ is the quark's helicity, $C_F = \frac{4}{3}$, $N_c = 3$, and p_1 and p_1' are the momenta of the quark incoming and outgoing, which have momentum fractions y_1 and y_1' , respectively, the latter being a fraction of $(1-z)p^+$. The incoming (outgoing) quark has charge e_1 (e_2). Diagrams 2(a) and 2(b) contribute equally to the e_1 terms and diagrams 2(c) and 2(d) contribute equally to the e_2 term. The calculation is gauge invariant. (Terms with an $\varepsilon \cdot q$ are dropped.) The integral I_π is

$$I_\pi = \int_0^1 \frac{d\xi_1}{\xi_2} \phi_\pi(\xi), \tag{10}$$

where ξ_i are momentum fractions of quarks in the pion and ϕ_π is the pion's distribution amplitude. The integral is the same as appears in the perturbative QCD calculation²⁻⁴ of the pion electromagnetic form factor

$$F_\pi(Q^2) = (16\pi\alpha_s C_F / Q^2) I_\pi^2. \tag{11}$$

Results for π^+ .— We must imbed the quark distribution amplitude \mathcal{M}_q between nucleon states. We will keep only the three-quark part of the wave function with the quark momentum fraction and transverse momentum dependences factorizing. We take P_{3q} , the probability of having the three-quark Fock component, equal to 1, to compensate for omitting the remaining Fock components. A simple form for the momentum fraction dependence is

$$\phi_N(\{y_i\}) = N_\phi (y_1 y_2 y_3)^\eta, \tag{12}$$

where y_1, y_2 , and y_3 are quark momentum fractions. We shall study below the sensitivity to varying the wave function, by varying η from (say) $0.6 \leq \eta \leq 1$ and using more sophisticated wave functions based upon results from QCD sum-rule analyses.

For the π^+ the interest is to compare the PQCD diagrams to the pole diagrams. The latter are dominated by the t -channel diagram, which is an order of magnitude bigger than the s -channel diagram. The pion pole diagram, Fig. 1(t), gives

$$\mathcal{M}_{\text{pole}} = (2\lambda_p) \left(\frac{8}{1-z} \right)^{1/2} \frac{zm_N \varepsilon \cdot p_\pi}{t - m_\pi^2} g_{\pi NN}(t) F_\pi(Q^2). \tag{13}$$

TABLE I. The ratio $R = \mathcal{M}_{\text{PQCD}}/\mathcal{M}_{\text{pole}}$ for several different nucleon distribution amplitudes. We feature the King-Sachrajda (KS) nucleon distribution amplitude, and give R using $g_{\pi NN}(t)$ from Eq. (4). The effect of $g_{\pi NN}$ may be seen from the column with $g_{\pi NN}$ divided out. Results for other distribution amplitudes are given as ratios to the results of using the KS one. The calculations are done in the limit of large ν ; if Q^2 , W , and t are given, they correspond to real cases of data from Ref. 1. Units for Q^2 , W , and t are appropriate powers of GeV.

z	Q^2	W	$-t$	$R(\text{KS})$	$\frac{R(\text{KS})g_{\pi NN}(0)}{g_{\pi NN}(t)}$	$\frac{R(\text{CZ})}{R(\text{KS})}$	$\frac{R(\text{GS})}{R(\text{KS})}$	$\frac{R(\eta=1)}{R(\text{KS})}$	$\frac{R(\eta=0.6)}{R(\text{KS})}$
0.10			0.01	0.18	0.17	0.51	1.05	1.14	1.51
0.25	1.94	2.67	0.07	0.12	0.08	0.83	-0.18	2.70	3.51
0.35	3.33	2.63	0.17	0.18	0.08	1.13	-1.68	3.62	4.88
0.48	6.30	2.66	0.43	0.81	0.22	0.78	-1.41	1.63	2.41
0.60	9.77	2.63	0.87	2.82	0.44	0.56	-0.64	0.72	1.23

(The s , t , and u graphs together are gauge invariant if form factors are omitted. Problems upon including form factors are well known and we will not describe them.¹¹) We present Table I, which gives the ratio $\mathcal{M}_{\text{PQCD}}/\mathcal{M}_{\text{pole}}$ at large ν and Q^2 for selected nucleon wave functions. The z and t are appropriate for the nearly zero center-of-mass photon-pion angle used by the experimenters. The PQCD graphs with our kinematics are for slightly larger angle, but with no pole in t ; the PQCD graphs are not strongly dependent on this angle (and can be made to match the experimental conditions by introducing a small transverse momentum to the active quark¹⁰). The wave functions are those of Chernyak and Zhitnitsky¹² (CZ), King and Sachrajda¹³ (KS), Gari and Stefanis¹⁴ (GS), and the $\eta=1$ given earlier. (The CZ distribution amplitude is based on results from QCD sum rules, KS is the same but corrects some numerical errors in the CZ work, and GS satisfies most of the QCD sum rules but gives a much smaller magnetic form factor for the neutron than KS or CZ.) The presented calculations are for longitudinally polarized photons, which give the largest amplitudes for pion production for both the pole and PQCD calculations. For I_π we use the Chernyak-Zhitnitsky result,³

$$I_\pi = \frac{5}{3} f_\pi \sqrt{3}/2, \quad (14)$$

which is $\frac{5}{3}$ the result valid²⁻⁴ for superhigh Q^2 .

With increasing z , the PQCD diagrams become more important relative to the pole diagrams with or without $g_{\pi NN}(t)$, and with the $g_{\pi NN}(t)$ given earlier the effect is quite dramatic. There are typically 20% corrections to

the pole diagram for z below 0.4, and for z above a half the PQCD diagrams dominate. For the Gari-Stefanis wave function there are interesting sign changes, leading to further questions about the destructive or constructive nature of the interference.

Results for π^0 .—The contributions of the pole diagrams here are very small. Not only is the t -channel diagram absent but the leading terms of the s - and u -channel diagrams cancel (for $m_\pi \rightarrow 0$, $z \approx x$, and $|t| \ll Q^2$). Further, we have calculated diagrams like Fig. 1(t) but with ω^0 or ρ^0 intermediate mesons; their contribution is small for longitudinal incoming photons. We are left with the PQCD diagram contributions to π^0 production, which are roughly comparable to π^+ production. This is presented more precisely in Table II, which gives the ratio of π^0/π^+ production for various z and various nucleon distribution amplitudes. Thus for moderate to high momentum transfers, we expect the production of the neutral meson to be comparable to that of the charged meson. This will be a test for the importance of the PQCD diagrams, which may be further validated by examining the Q dependence at fixed z . One will measure some nucleon integrals times the pion wave-function integral I_π , which also appears in the expression for the pion electromagnetic form factor.

Consider our perturbative QCD formulas further. For a given initial quark, the diagrams of Fig. 2 add with the same sign for a π^0 and partly cancel for the π^+ . In particular, the constructive addition of 2(b) and 2(c) for neutral mesons is unexpected if one observes their topological similarity to the meson pole diagram: the meson

TABLE II. Ratios of π^0/π^+ production for various z and various nucleon distribution amplitudes, from the PQCD diagrams only; z and t are given for the $p_{\pi\tau} = q_\tau$ kinematics.

z	$-t$	$\frac{\pi^0}{\pi^+}(\text{KS})$	$\frac{\pi^0}{\pi^+}(\text{CZ})$	$\frac{\pi^0}{\pi^+}(\text{GS})$	$\frac{\pi^0}{\pi^+}(\eta=1)$	$\frac{\pi^0}{\pi^+}(\eta=0.6)$
0.10	0.01	0.77	0.91	0.16	1.07	0.95
0.24	0.07	0.96	1.39	6.58	0.77	0.71
0.38	0.20	0.57	1.72	1.06	0.65	0.62
0.54	0.56	0.85	1.40	0.98	0.58	0.56
0.68	1.27	0.67	1.09	1.85	0.54	0.53

pole diagram proportional to the charge of the whole meson. The sign change from what one might naively expect is due to the hard gluon being timelike in diagrams 2(a) and 2(b) but spacelike in diagrams 2(c) and 2(d).

We can expect dominance of the PQCD diagrams to hold for other neutral mesons, meaning that production of $K^0, \eta^0, \rho^0, \dots$ will produce results given by known kinematic factors times some nucleon integrals times $I_K, I_\eta, I_\rho, \dots \equiv I_M$. If we take ratios of other neutral meson production to π^0 production at the same z , we can get the ratios I_M/I_π . In each case I_M is related to the meson's electromagnetic form factor, so that we have an indirect way of measuring the meson's electromagnetic form factor. Also, in each case there is a prediction for I_M based on QCD sum rules^{3,15} which can be verified or falsified. (One should note that the QCD sum-rule prediction for I_M is not complete, but that the indirect electromagnetic form-factor measurement should be valid even if the prediction for I_M is not.)

To summarize, (i) for the π^+ diagrams and high Q^2 at present experimental conditions, a soft $g_{\pi NN}(t)$ has significant effect. Since one uses these diagrams to get the pion electromagnetic form factor from data, significant changes—increases—in the extracted $F_\pi(Q^2)$ are induced.

(ii) Additionally, for π^+ electroproduction the PQCD diagrams compete with the pion and nucleon pole diagrams. At lower $|t|$ (where z is approximately x) the pole diagrams still dominate, with the PQCD diagrams being typically 20% as large in amplitude. At larger $|t|$ the PQCD contributions are larger than the pole diagrams. If the relative sign of the two contributions is positive, decreases in the extracted $F_\pi(Q^2)$ are induced.

(iii) More reliable measurements of F_π at high Q^2 require smaller $|t|$ and thus higher electron energy loss ν . For example, to get $|t|$ of 0.05 GeV² at Q^2 of 10 GeV² requires $\nu \approx 25$ GeV. This is, at least kinematically, possible at SLAC.

(iv) There will be significant π^0 production, particularly at higher $|t|$. This comes mainly from the PQCD diagrams, which give comparable amplitudes for π^0 and π^+ production. The pole diagram contribution to π^0 electroproduction is small.

(v) For neutral mesons generally, the PQCD diagrams give significant electroproduction. This provides an indirect way of measuring the form factors of the $K^0, \eta^0, \rho^0, \dots$. Vagaries associated with the nucleon wave functions can be eliminated by taking ratios of $K^0,$

η^0, ρ^0, \dots production to the π^0 at similar values of $|t|$. The measurements, particularly since they can be done at higher Q^2/ν , should be well suited to the capabilities of CEBAF.

We thank J. J. Napolitano for useful conversations. C.E.C. is supported by NSF Grant No. PHY-8911343 and J.M. by DOE Grant No. DE-FG05-88ER40435. C.E.C. also thanks NATO for a collaborative travel grant.

¹C. J. Bebek *et al.*, Phys. Rev. D **17**, 1693 (1978); C. N. Brown *et al.*, Phys. Rev. D **8**, 92 (1973).

²G. R. Farrar and D. R. Jackson, Phys. Rev. Lett. **43**, 246 (1979).

³V. L. Chernyak and A. R. Zhitnitsky, Phys. Rep. **112**, 173 (1984).

⁴G. P. Lepage and S. J. Brodsky, Phys. Rev. D **22**, 2157 (1980).

⁵W. R. Frazer, Phys. Rev. **115**, 1763 (1959); F. A. Berends, Phys. Rev. D **1**, 2590 (1970).

⁶S. J. Brodsky and G. R. Farrar, Phys. Rev. Lett. **31**, 1153 (1973); Phys. Rev. D **11**, 1309 (1975); V. A. Matveev, R. M. Muradyan, and A. V. Tavkhelidze, Lett. Nuovo Cimento **7**, 719 (1973).

⁷A. W. Thomas, Phys. Lett. **126B**, 97 (1983); Prog. Theor. Phys. Suppl. **91**, 204 (1987); Prog. Part. Nucl. Phys. **20**, 21 (1987); A. W. Thomas and K. Holinde, Phys. Rev. Lett. **63**, 2025 (1989).

⁸L. L. Frankfurt, L. Mankiewicz, and M. I. Strickman, Z. Phys. A **334**, 343 (1989).

⁹The purely quark part of these diagrams is used in the discussion of the quark breakup function by E. L. Berger and S. J. Brodsky, Phys. Rev. Lett. **42**, 940 (1979); E. L. Berger, Phys. Lett. **89B**, 241 (1980); Z. Phys. C **4**, 289 (1980).

¹⁰For the data point $Q^2=3.33$ GeV² and $W=2.63$ GeV, the active quark need only absorb about 150 MeV of transverse momentum for the photon-pion center-of-mass angle to be zero. This is well below the expected rms momentum of a quark in a proton, and similar statements can be made for the other data points of Ref. 1.

¹¹See, for example, F. Gross and D. O. Riska, Phys. Rev. C **36**, 1928 (1987).

¹²V. L. Chernyak and I. R. Zhitnitsky, Nucl. Phys. **B246**, 52 (1984); and Ref. 3.

¹³I. D. King and C. T. Sachrajda, Nucl. Phys. **B279**, 785 (1987).

¹⁴M. Gari and N. G. Stefanis, Phys. Lett. B **175**, 462 (1986); Phys. Rev. D **35**, 1074 (1987).

¹⁵V. L. Chernyak, A. R. Zhitnitsky, and I. R. Zhitnitsky, Nucl. Phys. **B204**, 477 (1982).